Pergamon

Int. J. Solids Structures Vol. 34, No. 5, pp. 591–602, 1997
Published by Elsevier Science Ltd
Printed in Great Britain.
0020-7683/96 $15.00 + .00

PII: S0020-7683(96)00033-9

SCATTERING OF A PLANE ACOUSTIC WAVE BY A SPHERICAL ELASTIC SHELL NEAR A FREE SURFACE

H. HUANG
Naval Surface Warfare Center, Indian Head Division, White Oak, Silver Spring, MD 20903-5640, U.S.A.

and

G. C. GAUNAURD
Naval Surface Warfare Center, Carderock Division, White Oak, Silver Spring, MD 20903-5640, U.S.A.

(*Received* 31 *May* 1995; *in revised form* 13 *February* 1996)

Abstract The acoustic scattering by a submerged spherical elastic shell near a free surface, which is insonified by plane waves at arbitrary angles of incidence is analyzed in an exact fashion using the classical separation of variables technique. To satisfy the boundary conditions at the free surface as well as on the surface of the spherical elastic shell, the mathematical problem is formulated using the image method. The scattered wave fields are expanded in terms of the classical modal series of spherical wave functions utilizing the translational addition theorem. Quite similar to the problem of scattering by multiple spheres, numerical computation of the scattered wave pressure involves the solution of an ill-conditioned complex matrix system the size of which depends on how many terms of the modal series are required for convergence. This in turn depends on the value of the frequency, and on the proximity of the spherical elastic shell to the free surface. The ill-conditioned matrix equation is solved using the Gauss Seidel iteration method and Twersky's method of successive iteration cross checking each other. Backscattered echoes from the spherical elastic shell are extensively calculated and displayed. The result also demonstrates that the large amplitude low frequency resonances of the echoes of the submerged elastic shell shift upward with proximity to the free surface. This can be attributed to the decrease of added mass for the shell vibration. The present benchmark solution could eventually be used to validate those found by numerical schemes. Published by Elsevier Science Ltd.

INTRODUCTION

The scattering of sound waves by bodies near a free surface presents difficulties and characteristics far beyond those present when the body is in a boundless space. The backscattering cross-section of a body near the sea surface, even when the sea is perfectly calm, often bears no resemblance to its cross-section in deep waters, far away from any environmental boundary. For the case of an impenetrable (i.e. soft, hard, perfectly conducting,etc....) body near a plane boundary, there have been some studies, both in the electromagnetic and in the acoustic literatures that have addressed some aspects of the multiple scattering problem that results (Brunning and Lo, 1971; Gaunaurd and Huang, 1994; Ivanov, 1968; Liang and Lo, 1967). When the body is an elastic structure, we know of no instance in which a detailed treatment has been published. The present paper studies the 3-dimensional scattering by an elastic spherical shell submerged near the free surface of an acoustic half-space, when the shell is insonified by a plane wave at an arbitrary angle of incidence. This steady-state formulation rests on the venerable method of separation of variables and the classical method of images. In view of the presence of the image, this becomes a multiple scattering problem truly of structural acoustics, since the scatterer and its image are both elastic shells. Our exact analytical solution generated within the context of linear acoustics is evaluated and graphically displayed in wide frequency bands that extend into the 'resonance region' of the shell. The shell theory used is the popular bending theory (Junger and Feit, 1972). This shell theory yields results that agree well with those of

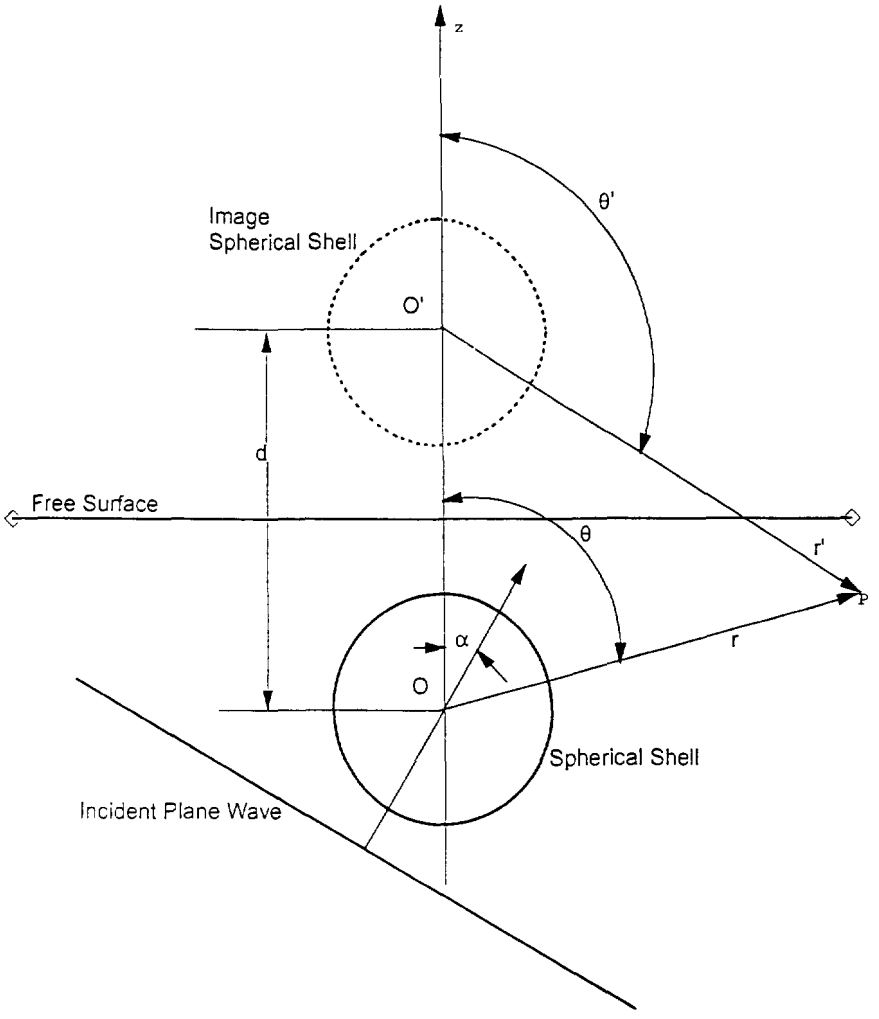

Fig. 1. Geometry of the problem.

the 3-dimensional theory of elasticity, for the shell thickness, material, and the frequency band we have used here. We also found that the large amplitude low frequency resonances of the echoes of the submerged elastic shell shift upward with proximity to the free surface. This can be attributed to the decrease of added mass for the shell vibration. The present solution could eventually serve to validate those found by numerical schemes.

DESCRIPTION OF THE PROBLEM

Figure 1 illustrates the geometry of the problem. The spherical elastic shell is located beneath the free surface. Its middle surface radius and thickness are denoted by a and h, respectively. Its material properties are mass density ρ_s, Young's modulus E and Poisson's ratio ν. The origin O of a spherical coordinate system (r, θ, φ) coincides with the center of the spherical shell. The azimuthal coordinate φ is not shown in the figure. The distance from O to the free surface is $d/2$. The line joining the two apexes of the spherical shell is perpendicular to the free surface. The mass density and sound speed of the fluid medium in which the shell is submerged are denoted by ρ and c, respectively. The propagation vector of the incident plane wave is parallel to the plane of the paper and makes an angle α with the normal to the free surface.

The image of the spherical shell mirrored by the free surface lies above the free surface. The origin O' of a second spherical coordinate system (r', θ', φ) also coincides with the center of the image spherical shell. The primed and the unprimed spherical coordinate

systems have identical azimuthal coordinate φ. The distance from O' to the free surface is also $d/2$.

The incident plane wave will be reflected by the free surface and this reflected wave plays the role of a second incident plane wave of the same magnitude, but is incident upon the spherical shell at a different angle. Moreover, the waves scattered by the vibrating elastic shell will also be reflected by the free surface and they will act as a third set of waves incident upon the shell. To completely determine the scattered wave field and the echo from the spherical elastic shell, the wave equation governing the wave motion in the fluid medium and the equation of motion of the shell are simultaneously solved satisfying the boundary conditions at the free surface and on the spherical elastic shell.

MATHEMATICAL FORMULATION

For clarity, the following dimensionless quantities are used:

$$W = \frac{w}{a}, \quad D = \frac{d}{a}, \quad R = \frac{r}{a}, \quad R' = \frac{r'}{a}, \quad \beta^2 = \frac{h^2}{12a^2},$$

$$M = \frac{\rho a}{\rho_s h}, \quad C^2 = \frac{E}{\rho_s(1-\nu)c^2}, \quad \Pi = \frac{p}{\rho c^2}, \quad \Omega = \frac{\omega a}{c}, \tag{1}$$

where w, ω and p denote, respectively, the radial deflection of the elastic shell, the angular frequency of the incident wave, and the pressure in the fluid medium. The Helmholtz equation governing the total pressure field in the fluid medium can be written as

$$\nabla^2\Pi + \Omega^2\Pi = 0 \tag{2}$$

where ∇^2 is the Laplacian and a time-dependence of $\exp(-i\Omega T)$ is assumed. The boundary conditions for Π are

$$\Pi = 0 \tag{3}$$

at the free surface and

$$\left(\frac{\partial\Pi}{\partial R}\right)_{R=1} = \Omega^2 W \tag{4}$$

on the spherical shell surface.

The mathematical expression for the incident plane wave depicted in Fig. 1 is (Ivanov, 1968)

$$\Pi^{in}(R, \theta, \varphi, \Omega) = e^{i\Omega R[\cos\theta\cos\alpha + \sin\theta\sin\alpha\cos\varphi]} \tag{5}$$

where $i = \sqrt{-1}$. The series expansion of eqn (5) in terms of spherical wave functions is

$$\Pi^{in}(R, \theta, \varphi, \Omega) = 2\sum_{n=0}^{\infty}\sum_{m=0}^{m=n} i^n \frac{2-\delta_{0m}}{N_{nm}} j_n(\Omega R) P_n^m(\cos\theta) P_n^m(\cos\alpha)\, e^{im\varphi} \tag{6}$$

where j_n and P_n^m are respectively the spherical Bessel function of the first kind and the Legendre function.

$$N_{nm} = \frac{2(n+m)!}{(2n+1)(n-m)!} \tag{7}$$

and

$$\begin{aligned} \delta_{0m} &= 1, \quad \text{for} \quad m = 0 \\ &= 0, \quad \text{for} \quad m \neq 0. \end{aligned} \tag{8}$$

The free surface will reflect this plane compression wave as a tension wave which will be incident on the sphere at an angle of incidence $(\pi - \alpha)$. This reflected wave can be considered as the mirror image of the incident plane wave from beneath. Its mathematical expression in the primed spherical coordinates is

$$\Pi^{inc'}(R', \theta', \varphi, \Omega) = -\mathrm{e}^{ikR'[\cos\theta'\cos(\pi-\alpha) + \sin\theta'\sin(\pi-\alpha)\cos\varphi]}, \tag{9}$$

which can be expressed in the unprimed coordinate system as

$$\Pi^{inc'}(R, \theta, \varphi, \Omega) = -\mathrm{e}^{i\Omega R[\cos\theta\cos(\pi-\alpha) + \sin\theta\sin\alpha\cos\varphi]}\,\mathrm{e}^{i\Omega D\cos\alpha}. \tag{10}$$

The series expansion of the above equation is

$$\Pi^{inc'}(R, \theta, \varphi, \Omega) = -2\mathrm{e}^{i\Omega D\cos\alpha}\sum_{n=0}^{\infty}\sum_{m=0}^{m=n} i^n \frac{2-\delta_{0m}}{N_{nm}}(-1)^{n-m} j_n(\Omega R) P_n^m(\cos\theta) P_n^m(\cos\alpha)\,\mathrm{e}^{im\varphi}. \tag{11}$$

The sum of the above 'two' incident waves is

$$\Pi^{inc} + \Pi^{inc'} = 2\sum_{n=0}^{\infty}\sum_{m=0}^{m=n} i^n \frac{2-\delta_{0m}}{N_{nm}} j_n(\Omega R) P_n^m(\cos\theta)[1-(-1)^{n-m}\mathrm{e}^{i\Omega D\cos\alpha}] P_n^m(\cos\alpha)\,\mathrm{e}^{im\varphi}. \tag{12}$$

At the free surface, $2R\cos\theta = D$, the sum of eqns (5) and (10) vanishes, and it can also be numerically demonstrated that eqn (12) vanishes there too. The wave scattered by the sphere is

$$\Pi^{sca}(R, \theta, \varphi, \Omega) = \sum_{n=0}^{\infty}\sum_{m=0}^{m=n} B_{nm} h_n(\Omega R) P_n^m(\cos\theta)\,\mathrm{e}^{im\varphi} \tag{13}$$

where the coefficients B_{nm} are to be determined from the boundary condition on the shell surface and h_n denotes the spherical Hankel function. The reflection of this scattered wave by the free surface is the negative image of eqn (13),

$$\Pi^{sca'}(R', \theta', \varphi, \Omega) = -\sum_{n=0}^{\infty}\sum_{m=0}^{m=n} B_{nm} h_n(\Omega R') P_n^m(\cos(\pi-\theta'))\,\mathrm{e}^{im\varphi}. \tag{14}$$

The total pressure field is

$$\begin{aligned} \Pi(R, \theta, \varphi, \Omega) &= \Pi^{inc} + \Pi^{inc'} + \Pi^{sca} + \Pi^{sca'} \\ &= 2\sum_{n=0}^{\infty}\sum_{m=0}^{n} i^n \frac{2-\delta_{0m}}{N_{nm}} j_n(\Omega R) P_n^m(\cos\theta)[1-(-1)^{n-m}\mathrm{e}^{i\Omega D\cos\alpha}] P_n^m(\cos\alpha)\,\mathrm{e}^{im\varphi} \end{aligned}$$

$$+\sum_{n=0}^{t}\sum_{m=0}^{n} B_{nm}h_n(\Omega R)P_n^m(\cos\theta)\,e^{im\varphi}$$

$$-\sum_{q=0}^{t}\sum_{m=0}^{q}(-1)^{q-m}B_{mq}h_q(\Omega R')P_q^m(\cos\theta')\,e^{im\varphi}$$

$$=2\sum_{n=0}^{t}\sum_{m=0}^{n} i^{n-m}\frac{2-\delta_{0m}}{N_{mn}}j_n(\Omega R)P_n^m(\cos\theta)[1-(-1)^{n-m}e^{i\Omega D\cos\alpha}]P_n^m(\cos\alpha)\,e^{im\varphi}$$

$$+\sum_{n=0}^{t}\sum_{m=0}^{n} B_{nm}h_n(\Omega R)P_n^m(\cos\theta)\,e^{im\varphi}$$

$$-\sum_{q=0}^{t}\sum_{m=0}^{q}(-1)^{q-m}B_{mq}\sum_{n=0}^{t}Q'_{nmmq}(D,\pi)j_n(\Omega R)P_n^m(\cos\theta)\,e^{im\varphi}. \tag{15}$$

The addition theorem of spherical wave functions for the geometry described in Fig. 1 (Ivanov, 1968) has been applied to the last sum of eqn (15) to represent it in the unprimed spherical coordinates and the quantity Q' is

$$Q'_{nmmq}(D,\pi)=\frac{2i^{n-q}}{N_{mn}}\sum_{\sigma=|n-q|}^{n+q} i^{\sigma}(-1)^{\sigma}b_{\sigma}^{qmnm}h_{\sigma}(\Omega D) \tag{16}$$

where

$$b_{\sigma}^{qmnm}=(-1)^m\sqrt{\frac{(q+m)!(n+m)!}{(q-m)!(n-m)!}}(q,n,0,0/\sigma,0)(q,n,m,-m/\sigma,0). \tag{17}$$

The quantity $(j_1,j_2,m_1,m_2/j,m)$ in the above equation is a Clebsch–Gordan coefficient.

The modal expansion of the radial deflection of the shell is

$$W=\sum_{n=0}^{t}\sum_{m=0}^{n} W_{nm}P_n^m(\cos\theta)\,e^{im\varphi} \tag{18}$$

and the boundary condition on a spherical elastic shell can also be written as

$$\left.\frac{\partial\Pi_{nm}}{\partial R}\right)_{R=1}=\Omega^2 W_{nm}. \tag{19}$$

The bending theory equation of motion for the spherical elastic shell (Junger and Feit, 1972) is used here. It can be written in terms of only the radial deflection W as the following:

$$W_{nm}=\frac{[-\Pi_{nm}(1)]}{\Gamma_n}, \tag{20}$$

where, for a complete uniform spherical shell, Γ_n does not contain m, and

$$\Gamma_n=\frac{[\Omega^4-(A_n+C_n)\Omega^2+(A_nC_n-B_nD_n)]}{[M(C_n-\Omega^2)]},$$

$$A_n=C^2\left\{2+\beta^2 n(n+1)\frac{[n(n+1)-(1-\nu)]}{(1+\nu)}\right\},$$

$$B_n = C^2 n(n+1)\left\{1+\beta^2\frac{[n(n+1)-(1-\nu)]}{(1+\nu)}\right\},$$

$$C_n = C^2(1+\beta^2)\frac{[n(n+1)-(1-\nu)]}{(1+\nu)},$$

$$D_n = \frac{B_n}{n(n+1)}. \tag{21}$$

Applying the boundary condition in eqn (19) yields

$$B_{mm} - \left(\sum_{q=0}^{i}(-1)^{q-m}B_{mq}Q'_{nmmq}(R'_{sf},\theta'_{sf})\right)X_n(\Omega)$$

$$= -2i^n\frac{2-\delta_{0m}}{N_{mm}}X_n(\Omega)[1-(-1)^{n-m}e^{j\Omega D\cos\alpha}]P_n^m(\cos\alpha) \tag{22}$$

where

$$X_n(\Omega) = \frac{\Gamma_n j'_n(\Omega)+\Omega j_n(\Omega)}{\Gamma_n h'_n(\Omega)+\Omega h_n(\Omega)}. \tag{23}$$

If $(N+1)$ terms, i.e. $(q=0-N)$ are used, eqn (22) can be arranged into a complex matrix equation for each m as the following:

$$[\mathbf{\Lambda}](\mathbf{B}) = (\mathbf{S}) \tag{24}$$

where $\mathbf{\Lambda}$ is a $(N+1-m)$ by $(N+1-m)$ complex matrix, and $\mathbf{B}$ and $\mathbf{S}$ are $(N+1-m)$ complex vectors for each m. The elements of the matrix $\mathbf{\Lambda}$ are

$$\Lambda_{nn} = 1-Q'_{nnmm}(D,\pi)X_n(\Omega) \tag{25}$$

for diagonal elements, and

$$\Lambda_{nq} = -(-1)^{q-m}Q'_{nmmq}(D,\pi)X_n(\Omega) \tag{26}$$

for the off-diagonal elements. The elements of the vector $\mathbf{S}$ are

$$S_n = -\frac{2i^n(2-\delta_{0m})}{N_{nm}}X_n(\Omega)P_n^m(\cos\alpha)[1-(-1)^{n-m}e^{j\Omega D\cos\alpha}] \tag{27}$$

and the elements of the vector $\mathbf{B}$ are B_{nm}. In the matrix equation, n and q range from m to N. From this matrix equation, the complex coupled coefficients B_{mn} can be solved for, and then the total or the scattered pressure field can be computed. For very large R,

$$h_n(\Omega R) \to i^{(n+1)}\frac{e^{j\Omega R}}{\Omega R}. \tag{28}$$

The total far field scattered pressure expression can be simplified as

$$\Pi^{sca}(R,\theta,\varphi,\Omega)+\Pi^{scar}(R',\theta',\varphi,\Omega)=$$

$$\frac{e^{i\Omega R}}{\Omega R}\sum_{n=0}^{\infty}\sum_{m=0}^{n} i^{-(n+1)}B_{nm}\left[P_n^m(\cos\theta)-(-1)^{n-m}\frac{R}{R'}e^{i\Omega(R'-R)}P_n^m(\cos\theta')\right]e^{im\varphi}. \quad (29)$$

The form function is defined as the absolute value of

$$f_\infty(R,\theta,\varphi,\Omega)=2R[\Pi^{sca}(R,\theta,\varphi,\Omega)+\Pi^{scar}(R,\theta,\varphi,\Omega)]\,e^{-i\Omega R}. \quad (30)$$

NUMERICAL RESULTS AND DISCUSSION

The complex coefficients B_{nm} in eqn (22) are found by solving the truncated complex linear system, eqn (24), exactly. The truncation, i.e. the number of terms N used for the sums from $n=0$ to $n=N$ and $q=0$ to $q=N$ in eqns (15), (27) and (22), depends on the degree of accuracy required, the value of Ω and the complexity of the wave interaction picture. For each frequency, it is necessary to solve the complex equation, eqn (24), N times to find B_{nm} where m and n range from 0 to N. The sizes of the matrices are $(N+1-m)\times(N+1-m)$.

As in the case of scattering by a hard sphere near the free surface (Gaunaurd and Huang, 1994), the off-diagonal elements of the matrix $\mathbf{A}$ for typical cases are in general many orders of magnitude smaller than the diagonal elements. The matrix $\mathbf{A}$ is therefore severely ill-conditioned and the linear complex system in eqn (24) is not solvable using the Gaussian elimination type of procedures, but lends itself congenially to be solved by the Gauss–Seidel iteration technique. Notwithstanding the details, the present solution method is similar to that of Brunning and Lo (1971). The Gauss–Seidel method does not guarantee convergence (Hildebrand, 1956). In fact, in the present computation for cases where the elastic shell is very close to the free surface ($D<2.3$), the method diverges in the neighborhoods of some of the resonance frequencies. The present converged numerical results are computed to 8-digits accuracy, and the Gauss–Seidel technique requires more iterations for larger matrices and lower values of m. At low ms it requires about 25 and at high ms 2 or 3 iterations to converge to the required 8-digits accuracy. The Gauss–Seidel results are checked by those obtained by Twersky's method of successive iteration used in other multiple scattering problems (Twersky, 1952; Liang and Lo, 1967). In the application of this later method, the corresponding values for the case in which the shell is submerged in an infinite fluid medium are first used for B_{mq} in the sum of eqn (22) to calculate a second set of B_{mq}. The second set is again used in the sum to calculate a third set of B_{mq}. This iteration continues until the kth result agrees with the $(k+1)$th to the present 8-digit accuracy criterion. For converged results, both Gauss–Seidel and Twersky's methods agree with each other. The two methods diverge at the same places.

All subsequent numerical results are presented for the case of a steel shell with a thickness to radius ratio $h/a=0.03$ submerged in water and for an incident angle $\alpha=0.25\pi$. The observation point is at $R=100.0$, $\theta=1.25\pi$, and $\varphi=\pi$. Results are obtained for a large range of Ω ($\cong ka$) as well as D, the normalized distance of the spherical shell center to the center of the image shell. The values of the material properties used are such that $M=4.27984$ and $C^2=17.79133$. In the computations, $N=40$ is used for the results to converge to 8-digits accuracy up to $\Omega=25.0$.

It is due to the term Π^{scar}, eqn (14), representing the reflection of the scattered pressure radiated from the shell that the coefficients B_{nm} are coupled in n and consequently their values have to be calculated by solving the simultaneous complex system in eqn (22). Alternatively, it can be said that this is due to the repeated interactions between the real and the image spherical elastic shells. To facilitate the evaluation of the interaction effects due to the image spherical shell, the problem is first solved without the term Π^{scar} and the backscattered form function, eqn (30), based only on the scattered pressure emanating from the real shell, Π^{sca}, is first plotted. It is clear from eqns (22) and (16) that the interaction of the image spherical shell manifests itself through the term Q'_{nmmq} which is proportional

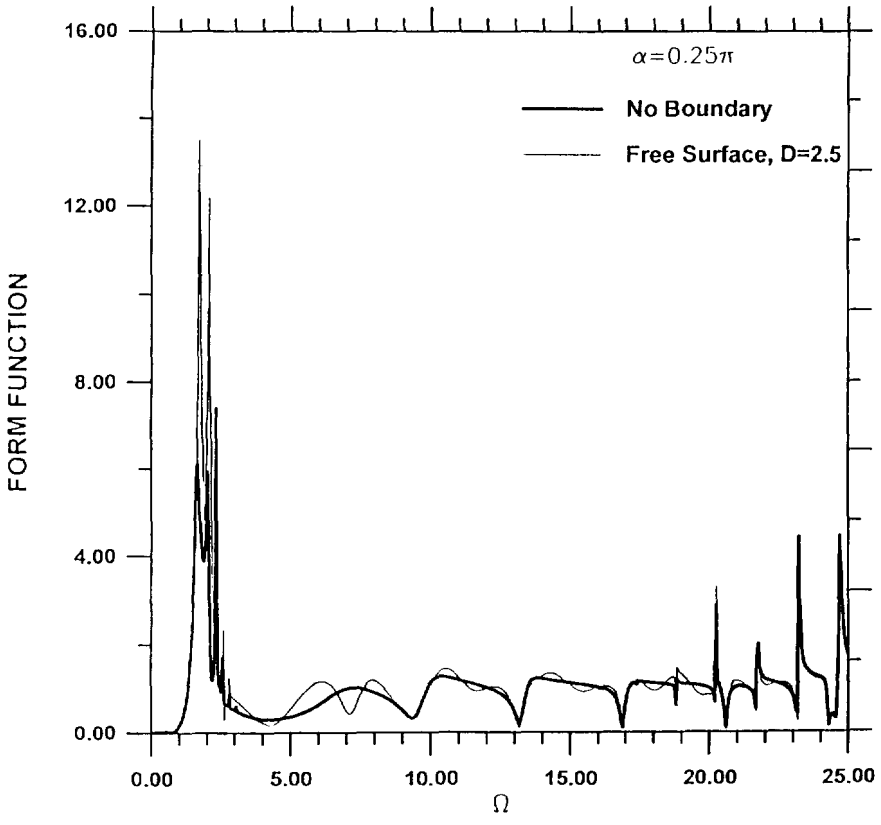

Fig. 2. Backscattering form function based on Π^{sc} only, without Π^{inc} in the solution, for $D = 2.5$.

to the spherical Hankel function $h_n(\Omega D)$ which in turn has a modulus decreasing with ΩD. It therefore follows that the interaction effects of the image spherical shell decrease either with higher frequencies or with larger distances of the shell from the free surface. In other words, the values of Π^{sc} would approach those for the scattering of a spherical elastic shell in an infinite boundless fluid medium as D or Ω is increased. The backscattered farfield form function is calculated at $R = 100.0$, $\theta = 1.25\pi$ and $\varphi = \pi$. Figure 2 presents this form function vs Ω (light solid curve) for the case where the apex of the spherical shell is 0.25 radius below the free surface ($D = 2.5$) and compares it to that of the same spherical shell in an infinite fluid medium (heavy solid curve). It can be seen that the difference between the two curves is very pronounced for the large amplitude low frequency resonances of the echoes of the submerged elastic shell and after $\Omega = 5.0$ the difference tapers off quickly with the increase of frequency. This demonstrates that the effect of the reflected scattered pressure radiated by a submerged elastic structure in close proximity to the free surface is significant. The resonance frequencies of the low frequency echoes shift upward as the shell is placed closer to the free surface. This is shown more clearly in Fig. 3 using an enlarged Ω axis scale. This frequency shift phenomenon has been measured and calculated for cases of vibrating bubbles near a free surface (Strasberg, 1953). Strasberg (1953) effectively reasoned that this frequency shift is due to the decrease of added mass of the vibrating object by the proximity of the free surface. From the fluid-structure interaction point of view, the effect of fluid added mass is quite significant for the low frequency vibrations of submerged elastic structures. By the same reasoning, it can be expected that the low resonance frequencies of a vibrating structure in the vicinity of a hard surface or another structure will shift downward due to the increase of added mass. The present numerical example is for a rather thick shell ($h/a = 0.03$). It is also expected that the frequency shift could be more pronounced for thinner shells.

The corresponding two curves for the case where the apex of the spherical shell is 4 radii beneath the free surface ($D = 10.0$) is presented in Fig. 4. Here the effect of the reflected scattered wave is insignificant on the magnitude of the form function. The effect

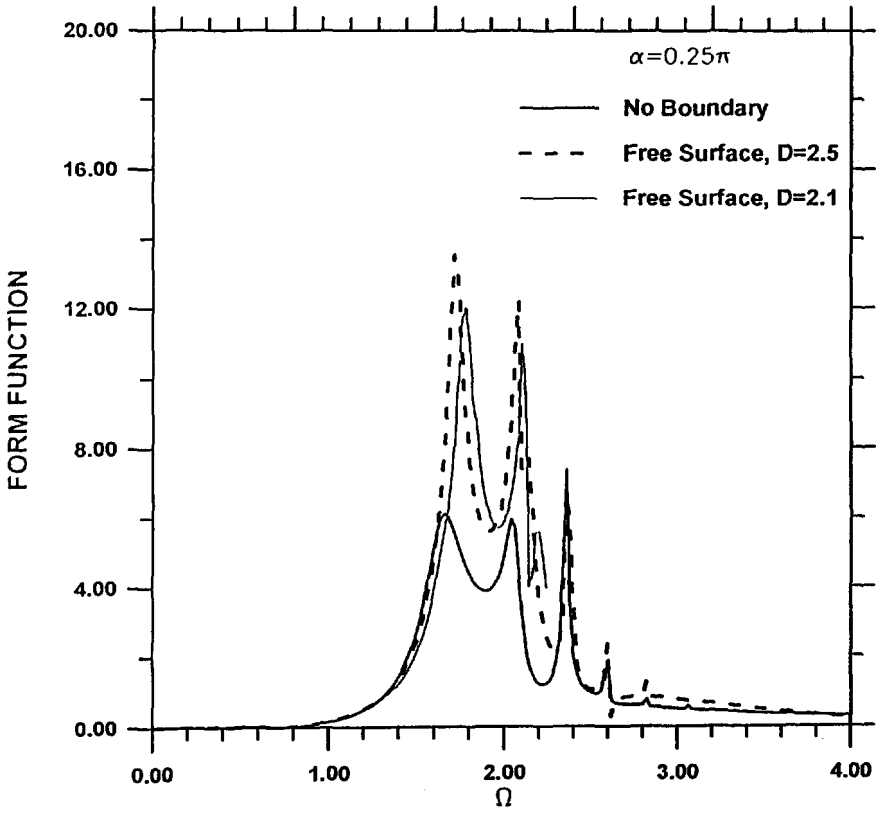

Fig. 3. Upward shifting of the low resonance frequencies of a vibrating spherical elastic shell submerged near the free surface.

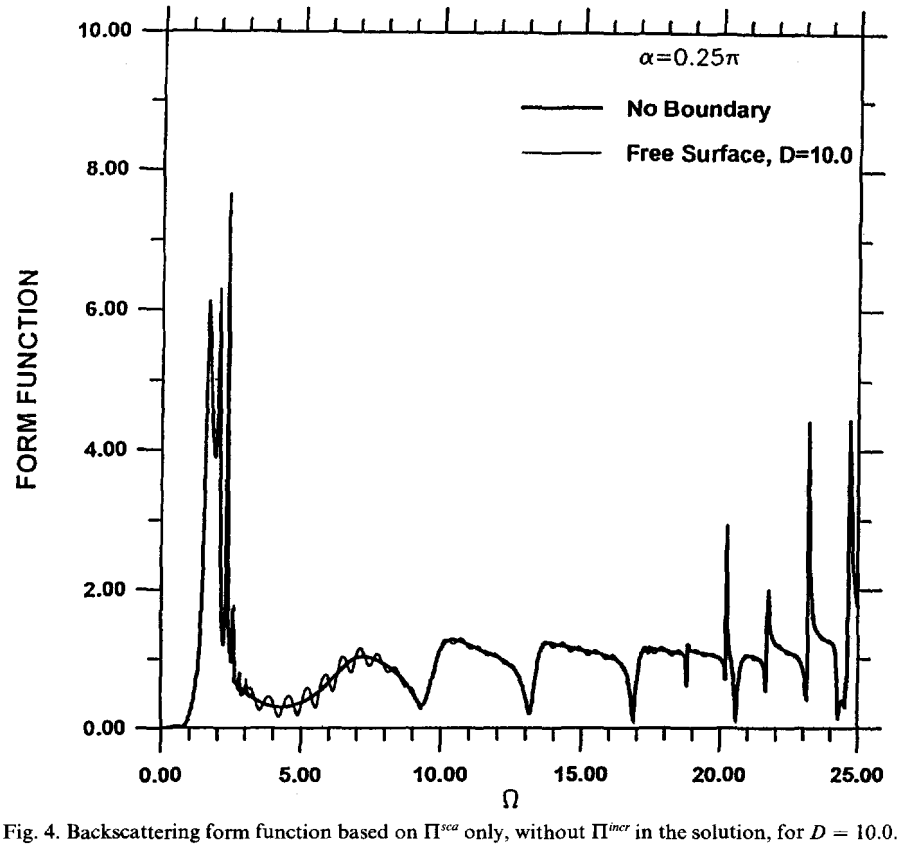

Fig. 4. Backscattering form function based on Π^{sca} only, without Π^{incr} in the solution, for $D = 10.0$.

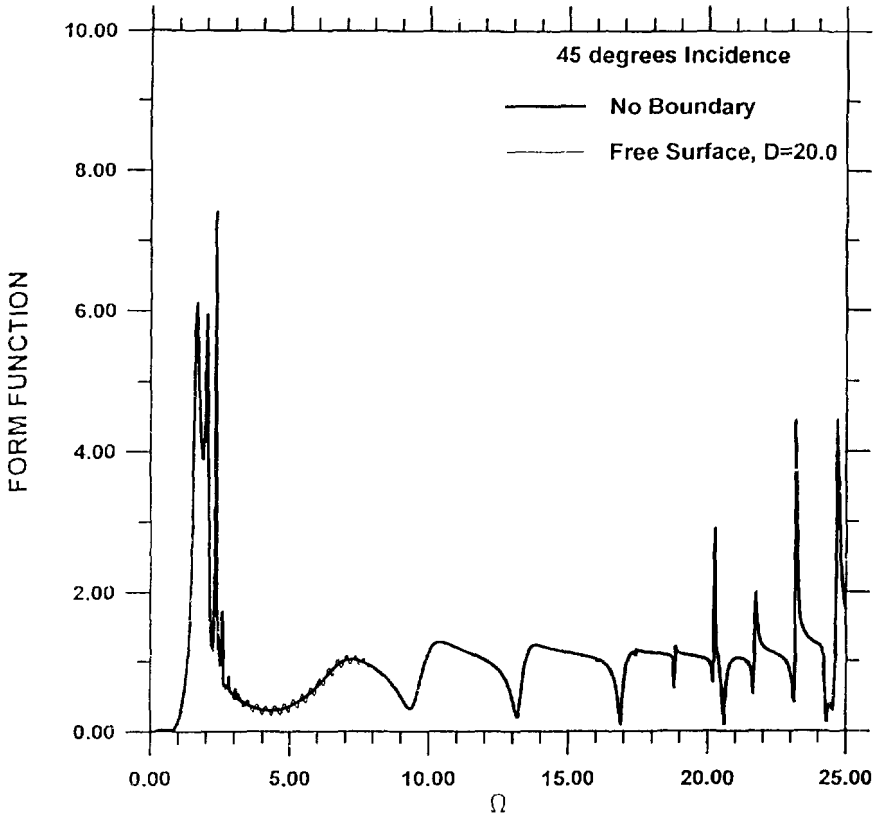

Fig. 5. Backscattering form function based on Π^{scat} only, without Π^{incr} in the solution, for $D = 20.0$.

forms an oscillation pattern due to the oscillating nature of $h_n(\Omega D)$ in the term Q'_{nmmq} at large ΩD as indicated in eqn (28). It is evident that the period of oscillation is $2\pi/D$. The same curves for the case in which the apex of the spherical shell is 9 radii beneath the free surface ($D = 20.0$) are plotted in Fig. 5 where it can be seen that the effect of the reflected scattered pressure is very small and yet the signal of this oscillation pattern is still quite clearly visible. Results for the case in which the apex of the spherical shell is 24 radii beneath the free surface ($D = 50.0$) are also computed and when plotted in the same scale as Fig. 5, the effect of the reflected scattered pressure is no longer visible.

Hereafter, the reflected incident wave Π^{incr} is included in the calculations. As indicated by eqns (10) and (29), there are phase factors $e^{i\Omega D\cos\gamma}$ and $e^{i\Omega(R' - R)}$ associated with Π^{incr} and Π^{scat}, respectively. In the time domain, these phase factors would imply different arrival times for these two waves. As discussed earlier, there are three sets of repeatedly incident waves acting on the spherical shell from different directions and with different phases, therefore the successive interactions among the various reflected and creeping waves are much more complex than in the infinite fluid medium case. Now the backscattering form functions are calculated based on the sum of $\Pi^{scat}+\Pi^{incr}$. Again, all backscattering form functions are presented for $\alpha = 0.25\pi$, $R = 100.0$, $\theta = 1.25\pi$ and $\varphi = \pi$. Figure 6 is a plot (light solid curve) for the case in which the shell is in close proximity of the free surface ($D = 2.5$) together with the corresponding form function (heavy solid curve) of the same shell in an infinite fluid medium. Here, as shown earlier in Fig. 2, the effect of the reflected scattered pressure is significant at low frequency. With the participation of the reflected incident plane wave, the magnitude of the echo averaged over frequency is roughly twice that of the infinite medium case.

Figure 7 plots the corresponding two curves for the case in which the shell is relatively far from the free surface ($D = 20.0$). Here, although the effect of the reflected scattered pressure is negligible as shown in Fig. 5, some of the low frequency resonance peaks are still twice the value of those for the infinite medium case due to the participation of the surface-reflected incident plane wave. The highly oscillatory pattern is due to the phase

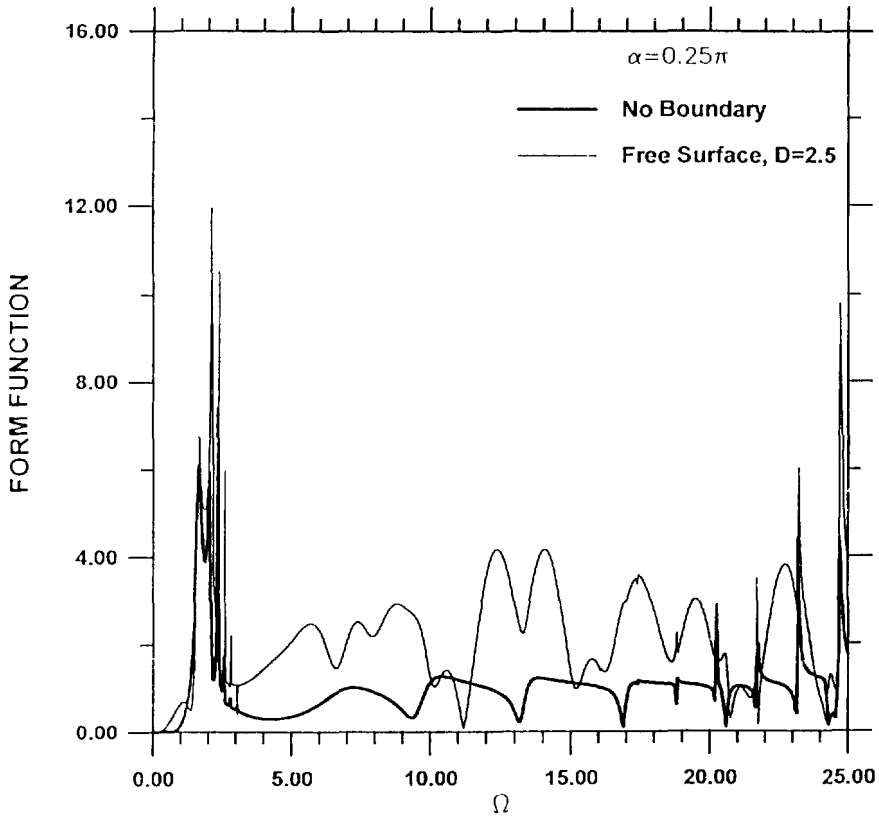

Fig. 6. Backscattering form function based on the sum of $\Pi^{(\infty)} + \Pi^{(s)}$, including $\Pi^{(ps)}$ in the solution, for $D = 2.5$.

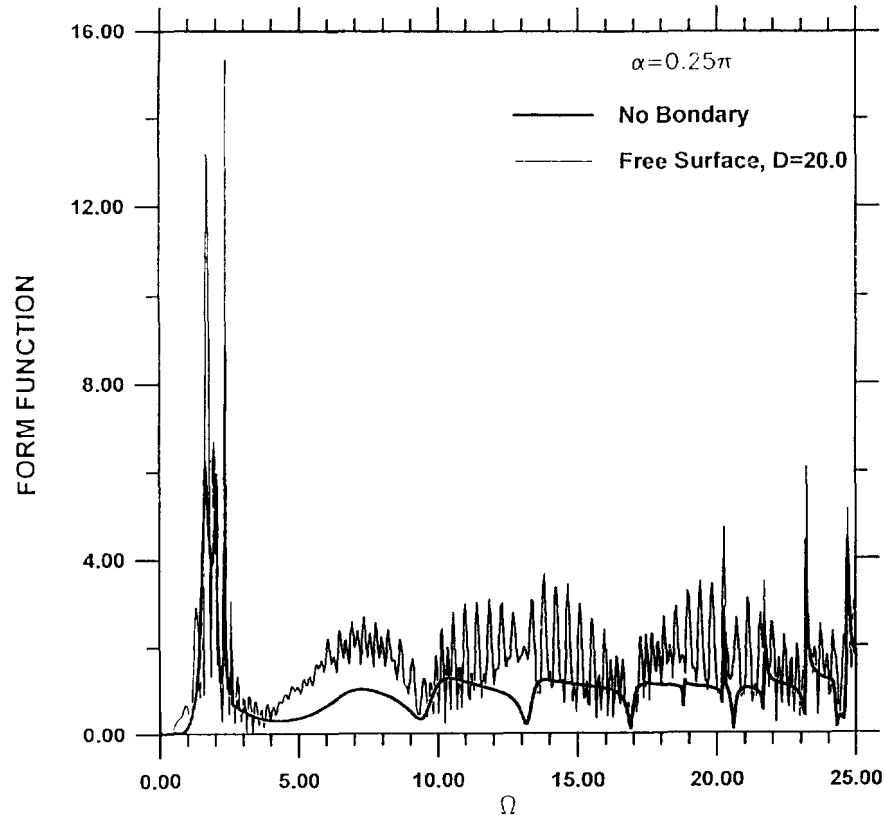

Fig. 7. Backscattering form function based on the sum of $\Pi^{(\infty)} + \Pi^{(s)}$, including $\Pi^{(ps)}$ in the solution, for $D = 20.0$.

factor $e^{i\Omega D\cos\gamma}$. This is the exact mathematical description of the Lloyd mirror effect of elementary acoustics (Urick, 1967). Almost the same form function curve in Fig. 7 can be obtained by a much simpler computation neglecting the sum on the left-hand side of eqn (22).

In summary, the present paper has presented an exact analytical solution based on modal series expansion for the title problem. This steady-state solution is obtained within the framework of linear acoustics and is valid everywhere except when the shell is touching the free surface. With minor modification, the mathematical formulation and numerical solution method can be immediately applied to solve the corresponding problem for the shell placed near a hard surface or for the scattering by two or more spherical elastic shells of different sizes and properties. The numerical results also demonstrate that the low resonance frequencies of a vibrating submerged structure shift upward with the proximity of the free surface. The present solution could eventually be used to validate those found by strictly numerical codes.

Acknowledgements The authors acknowledge the partial support of the Independent Research Program of the NSWC Carderock Division.

REFERENCES

Brunning, J. and Lo, Y. (1971). Multiple scattering of electromagnetic waves by spheres. Part I. Multipole expansion and ray-optical solutions. *IEEE Trans. Antennas Propag.* **AP-19,** 378–390.

Gaunaurd, G. C. and Huang, H. (1994). Acoustic scattering by a spherical body near a plane boundary. *J. Acoust. Soc. Am.* **96,** 2526–2536.

Hildebrand, F. B. (1956). *Introduction to Numerical Analysis.* Chap. 10, McGraw-Hill Book Company, Inc., NY.

Ivanov, Ye. (1968). *Diffraction of Electromagnetic Waves by Two Bodies.* Nauka, Tekhnika, Minsk (NASA Technical Translation #F-587 (1970)), pp. 121–127.

Junger, M. C. and Feit, D. (1972). *Sound, Structures, and Their Interaction.* Chap. 10, The MIT Press, Cambridge, Massachusetts.

Liang, C. and Lo, Y. T. (1967). Scattering by two spheres. *Radio Sci.* **2,** 1481–1495.

Strasberg, M. (1953). The pulsation frequency of nonspherical gas bubbles in liquids. *J. Acoust. Soc. Am.* **25,** 536–537.

Twersky, V. (1952). Multiple scattering of radiation by an arbitrary configuration of parallel cylinders. *J. Acoust. Soc. Am.* **24,** 42–46.

Urick, R. J. (1967). *Principles of Underwater Sound for Engineers.* McGraw-Hill Book Company, Inc., NY, pp. 112–123.